JOURNAL OF SOLID STATE CHEMISTRY 93, 69–76 (1991)

# A Layered Framework Characterized by Two Independent Tunnels: The Single Crystal Structure of Strontium Vanadium (III) Pyrophosphate, $SrV_2(P_2O_7)_2$

SHIOU-JYH HWU* AND EMILY D. WILLIS

*Department of Chemistry, Rice University, P.O. Box 1892,*
*Houston, Texas 77251*

Received December 14, 1990; in revised form March 5, 1991

The crystal structure of strontium vanadium (III) pyrophosphate, $SrV_2(P_2O_7)_2$, has been analyzed by the single crystal X-ray diffraction method. The title compound crystallizes in a triclinic ($P\bar{1}$) unit cell, with lattice dimensions: $a$ = 4.8006 (7) Å, $b$ = 7.117 (1) Å, $c$ = 7.8569 (8) Å, $\alpha$ = 89.92 (1)°, $\beta$ = 92.38 (1)°, $\gamma$ = 106.57 (1)°, $V$ = 257.05 (6) Å$^3$, and $Z$ = 1. The single crystal structure refinement gives a final structure solution with $R/R_w$ indexes on $F_0^2$ of 0.021/0.030 for 100 variables and GOF = 1.38. The layered type structural framework, built up from corner-sharing $VO_6$ octahedra and $P_2O_7$ pyrophosphate groups, possesses two types of tunnel structures of which the larger tunnels are occupied by strontium atoms. The strontium atoms are centered at the origin of the lattice and exhibit an irregular $SrO_{10}$ polyhedron which can be best described as a tetra-face-capped octahedron. The structure comparison with previously reported $BaTi_2(P_2O_7)_2$ and $Na_xMoP_2O_7$ ($0.25 \leq x \leq 0.50$) is also discussed.

## Introduction

Numerous structurally interesting compounds have been isolated during the study of reduced early transition metal ($M$) phosphate systems, $A$–M–P–O. It has been demonstrated that the electropositive cation ($A$: monovalent or divalent cations) plays an important role in not only stabilizing the low valent oxidation state of transition metal cations but also in governing the formation of transition metal phosphate frameworks (*1–4*). In the systems of $A^I$–$M$–P–O, where $A^I$ = alkali metal cations and $M$ = Ti, V, Mo, there is remarkable structural similarity among the compounds that are associated with trivalent ($M^{3+}$) cations. For example, several new titanium(III) pyrophosphates with a general formula of $A^ITiP_2O_7$, where $A^I$ = Li (*1*), Na (*2*), K, Rb, and Cs (*3*), are known to be isostructural with their corresponding vanadium and molybdenum analogues. Through the substitution of a divalent cation, e.g., $Ba^{2+}$, for the monovalent alkali metal cation, a new layered compound barium titanium(III) pyrophosphate, $BaTi_2(P_2O_7)_2$, was isolated (*4*). Attempts to synthesize the strontium and calcium analogues have yielded polycrystalline samples which show markedly different X-ray diffraction (XRD) patterns (*1*). To study the size effect in the structure formation of alkaline earth metal containing trivalent transition metal pyrophosphate series, research

---

* To whom correspondence should be addressed.

0022-4596/91 $3.00

on the system $A^{II}O$–$V_2O_3$–$P_2O_5$ ($A$ = Ba, Sr, and Ca) has been initiated. As expected, the isostructural compound $BaV_2(P_2O_7)_2$ ($a$ = 10.606 (3) Å, $b$ = 10.450 (3) Å, $c$ = 9.689 (2) Å, $\beta$ = 103.08 (2)°, and $V$ = 1046.1 (6) Å$^3$) was isolated (*5*). However, both Sr and $CaV_2(P_2O_7)_2$ form a different structure than that of the titanium analogues, according to the XRD patterns. In this paper, the synthesis and structure of $SrV_2(P_2O_7)_2$ and structure comparison to the previously reported barium titanium pyrophosphate (*4*) are discussed.

TABLE I

CRYSTALLOGRAPHIC DATA FOR $SrV_2(P_2O_7)_2$

| | |
|---|---|
| Formula mass (amu) | 537.39 |
| Space group | ($P\bar{1}$) (No. 2) |
| $a$ (Å) | 4.8006(7) |
| $b$ (Å) | 7.117(1) |
| $c$ (Å) | 7.8569(8) |
| $\alpha$ (degrees) | 89.92(1) |
| $\beta$ (degrees) | 92.38(1) |
| $\gamma$ (degrees) | 106.57(1) |
| $V$ (Å$^3$) | 257.05(6) |
| $Z$ | 1 |
| $T$ (K) of data collection | 296 |
| $\rho$ calc. (g cm$^{-3}$) | 3.47 |
| Radiation (graphite monochromated) | Mo$K\alpha$ ($\lambda$ = 0.71069 Å) |
| Crystal shape, color | Gem, yellowish green |
| Crystal size (mm) | 0.20 × 0.20 × 0.25 |
| Linear abs. coeff. (cm$^{-1}$) | 74.40 |
| Transmission factors | 0.70 ~ 1.00 |
| Scan type | $\omega - 2\theta$ |
| Scan speed (deg min$^{-1}$) | 4.0 |
| Scan range (deg.) | −0.45 to 0.45 in $\omega$ |
| Background counts | ¼ of scan range on each side of reflection |
| $2\theta$ (max) | 55° |
| Data collected | $\pm h$, $\pm k$, $\pm l$ |
| $p$ for $\sigma$ ($F^2$) | 0.01 |
| No. of unique data ($F_0^2 > 0$) | 1183 |
| No. of unique data with $F_0^2 > 3\sigma F_0^2$) | 1049 |
| $F_{000}$ | 256 |
| $R(F^2)/R_w(F^2)$/GOF | 0.021/0.030/1.38 |
| No. of variables | 100 |

## Experimental

*Syntheses.* Irregular shaped crystals of the strontium vandium(III) pyrophosphate $SrV_2(P_2O_7)_2$ were obtained in a reaction mixture of strontium vanadate, vanadium metal powder (Aldrich, 99.5%), and phosphorus pentaoxide (Mallinckrodt, 99.+%). Polycrystalline $Sr_2V_2O_7$ (*6*) was prepared by calcination of a stoichiometric amount of $SrCO_3$ (Johnson Matthey, 99.994%) and $V_2O_5$ (Aldrich 99.6%) at 900°C in air. The reduction reaction and the *in situ* crystal growth process were carried out in a fused silica tube with the reactant ratio of $Sr_2V_2O_7 : V : P_2O_5$ = 1 : 2 : 4. The reaction conditions have been previously reported (*4*). It was noticed that the quartz tube was seriously attacked and a contaminated reaction product of a structurally known compound $VO(SiP_2O_8)$ (*7*) was found along the inner wall. However, the major reaction product was yellowish green crystals of $SrV_2(P_2O_7)_2$ in ca. 60% yield. In order to avoid the quartz contamination, the stoichiometric reaction product of the title phase was synthesized at a lower temperature, 800°C. The resultant green polycrystalline material was in high yield (>95% purity), according to the XRD powder patterns.

*Single crystal X-ray structure determination.* A transparent yellowish green crystal, with average dimensions 0.20 × 0.20 × 0.25 mm, was selected for single crystal X-ray structure determination. Indexing and intensity data collection were performed on a Rigaku AFC5S four-circle diffractometer (Mo$K\alpha$ radiation, $\lambda$ = 0.71069 Å) equipped with a graphite monochrometer. Detailed crystallographic parameters are tabulated in Table I. The unit cell parameters and the orientation matrix for data collection were determined by a least-squares fit of 25 peak maxima, 7° < $2\theta$ < 24°. There was no detectable decay in intensity profiles according to three standard reflections (1,0,1,; 1,−1,1; 0,0,1) which were measured every 100 reflections during data collection. Three azimuthal scans ($2\theta$ = 18.76°, 23.28°, 28.24°) were used for absorption corrections. The atomic coordinates were found using the di-

TABLE II

POSITIONAL AND THERMAL PARAMETERS FOR $SrV_2(P_2O_7)_2$

| Atom | Atomic parameters | | | |
|---|---|---|---|---|
| | $x$ | $y$ | $z$ | $B_{eq}(Å^2)$[a] |
| Sr | 0 | 0 | 0 | 1.13(2) |
| V(1) | 0 | 0 | $\frac{1}{2}$ | 0.41(2) |
| V(2) | $\frac{1}{2}$ | $\frac{1}{2}$ | 0 | 0.44(2) |
| P(1) | 0.6187(2) | 0.2283(1) | 0.7025(1) | 0.49(2) |
| P(2) | 0.0304(2) | 0.6172(1) | 0.7529(1) | 0.46(2) |
| O(1) | 0.5155(5) | 0.2388(3) | 0.8842(3) | 0.74(7) |
| O(2) | 0.8218(5) | 0.0971(3) | 0.7059(3) | 0.70(7) |
| O(3) | 0.3793(5) | 0.1753(3) | 0.5678(3) | 0.84(7) |
| O(4) | 0.8048(5) | 0.4442(3) | 0.6494(3) | 0.70(7) |
| O(5) | 0.8796(5) | 0.6492(3) | 0.9155(3) | 0.70(7) |
| O(6) | 0.6976(5) | 0.4423(3) | 0.2072(3) | 0.81(7) |
| O(7) | 0.9110(5) | 0.1990(3) | 0.3486(3) | 0.94(8) |

| Atom | Thermal parameters[b] | | | | | |
|---|---|---|---|---|---|---|
| | $U_{11}$ | $U_{22}$ | $U_{33}$ | $U_{12}$ | $U_{13}$ | $U_{23}$ |
| Sr | 0.0212(3) | 0.0071(2) | 0.0130(2) | 0.0016(2) | −0.0016(2) | 0.0003(2) |
| V(1) | 0.0055(3) | 0.0046(3) | 0.0053(3) | 0.0011(3) | 0.0001(3) | 0.0002(3) |
| V(2) | 0.0056(3) | 0.0053(3) | 0.0060(3) | 0.0018(3) | 0.0006(3) | 0.0006(3) |
| P(1) | 0.0062(4) | 0.0055(4) | 0.0063(4) | 0.0008(3) | 0.0012(3) | −0.0005(3) |
| P(2) | 0.0059(4) | 0.0054(4) | 0.0061(3) | 0.0016(3) | 0.0005(3) | 0.0004(3) |
| O(1) | 0.013(1) | 0.008(1) | 0.008(5) | 0.0034(8) | 0.0037(9) | 0.0007(8) |
| O(2) | 0.010(1) | 0.011(1) | 0.007(1) | 0.0048(9) | 0.0016(8) | 0.0000(8) |
| O(3) | 0.008(1) | 0.010(1) | 0.012(1) | −0.0002(8) | −0.0008(9) | 0.0001(9) |
| O(4) | 0.010(1) | 0.007(1) | 0.008(1) | −0.0013(8) | 0.0014(8) | 0.0007(8) |
| O(5) | 0.007(1) | 0.010(1) | 0.009(1) | 0.0016(8) | 0.0023(8) | −0.0012(8) |
| O(6) | 0.009(1) | 0.015(1) | 0.009(1) | 0.0068(9) | −0.0002(9) | 0.0015(9) |
| O(7) | 0.012(1) | 0.008(1) | 0.016(1) | 0.0021(9) | −0.000(1) | 0.0050(9) |

[a] Anisotropically refined atoms are given in the form of the isotropic equivalent displacement parameter defined as $B_{eq} = \frac{4}{3}[a^2\beta_{11} + b^2\beta_{22} + c^2\beta_{33} + (2ab\cos\gamma)\beta_{12} + (2\,ac\cos\beta)\,\beta_{13} + (2\,bc\cos\alpha)\,\beta_{23}]$.

[b] The general temperature-factor expression of an atom for a given set of planes ($hkl$) is $\exp[-2\pi^2(U_{11}h^2a^{*2} + U_{22}k^2b^{*2} + U_{33}l^2c^{*2} + 2\,U_{12}hla^*b^*\cos\gamma^* + 2\,U_{13}hla^*c^*\cos\beta^* + 2\,U_{23}\,klb^*c^*\cos\alpha^*)]$, where the $U_{ij}$ are the thermal parameters expressed in terms of mean-square amplitudes of vibration in angstroms.

rect method, and the structure and thermal parameters were refined by full-matrix least-squares methods, as described in Ref. (*4*), based on $F^2$ to $R = 0.021$, $R_w = 0.030$, and GOF = 1.38. The occupancy factor for strontium atoms was initially refined. The resultant value suggested full occupancy. The final positional and thermal parameters are given in Table II and the selected bond distances and angles are listed in Table III.

## Structure Description and Discussion

As shown in Fig. 1, the framework of $SrV_2(P_2O_7)_2$ is built up from corner-sharing $VO_6$ octahedra and $P_2O_7$ pyrophosphate

TABLE III

IMPORTANT BOND DISTANCES (Å) AND ANGLES (deg) FOR $SrV_2(P_2O_7)_2$

| | | | | | |
|---|---|---|---|---|---|
| | | $VO_6$ octahedra | | | |
| V(1)–O(2) | 2.069(2) | (2×) | V(2)–O(1) | 2.092(2) | (2×) |
| V(1)–O(3) | 1.944(2) | (2×) | V(2)–O(5) | 1.971(2) | (2×) |
| V(1)–O(7) | 1.975(2) | (2×) | V(2)–O(6) | 1.952(2) | (2×) |
| O(2)$^a$–V(1)–O(3)$^b$ | | 89.83(9) | O(1)$^e$–V(2)–O(5)$^f$ | | 86.94(9) |
| O(2)$^c$–V(1)–O(7)$^a$ | | 87.72(9) | O(1)$^f$–V(2)–O(6)$^g$ | | 88.48(9) |
| O(3)$^d$–V(1)–O(7)$^a$ | | 88.07(9) | O(5)$^f$–V(2)–O(6)$^d$ | | 89.34(9) |
| O(2)$^a$–V(1)–O(2)$^c$ | | 180.00 | O(1)$^e$–V(2)–O(1)$^f$ | | 180.00 |
| O(3)$^b$–V(1)–O(3)$^d$ | | 180.00 | O(5)$^e$–V(2)–O(5)$^f$ | | 180.00 |
| O(7)$^a$–V(1)–O(7)$^c$ | | 180.00 | O(6)$^d$–V(2)–O(6)$^g$ | | 180.00 |
| | | $PO_4$ tetrahedra | | | |
| P(1)–O(1) | | 1.540(2) | P(2)–O(4) | | 1.588(2) |
| P(1)–O(2) | | 1.530(2) | P(2)–O(5) | | 1.543(2) |
| P(1)–O(3) | | 1.495(2) | P(2)–O(6) | | 1.504(2) |
| P(1)–O(4) | | 1.606(2) | P(2)–O(7) | | 1.494(2) |
| O(1)–P(1)–O(2) | | 108.0(1) | O(4)–P(2)–O(5) | | 106.3(1) |
| O(1)–P(1)–O(3) | | 114.5(1) | O(4)–P(2)–O(6) | | 108.6(1) |
| O(1)–P(1)–O(4) | | 108.5(1) | O(4)–P(2)–O(7) | | 109.5(1) |
| O(2)–P(1)–O(3) | | 114.6(1) | O(5)–P(2)–O(6) | | 112.1(1) |
| O(2)–P(1)–O(4) | | 107.7(1) | O(5)–P(2)–O(7) | | 107.9(1) |
| O(3)–P(1)–O(4) | | 103.2(1) | O(6)–P(2)–O(7) | | 112.2(1) |
| | | P(1)–O(4)–P(2) | 132.5(1) | | |

*Note.* Symmetry codes: $a = 1-x, -y, 1-z$; $b = -x, -y, 1-z$; $c = -1+x, y, z$; $d = x, y, z$; $e = 1-x, 1-y, 1-z$; $f = x, y, -1+z$; $g = 1-x, 1-y, -z$.

groups. Each of the pyrophosphate groups consists of two $PO_4$ tetrahedra sharing a corner oxygen atom. The structural framework possesses two different sizes of tunnels. The larger tunnel (T1) is characterized by four $VO_6$ octahedra and four $PO_4$ tetrahedra (4O + 4T; as shown in Fig. 2a) and is occupied by the counter cation, $Sr^{2+}$, at (0,0,0). The smaller empty tunnel (T2) is centered at $(0,\frac{1}{2},\frac{1}{2})$ by 2O + 4T (Fig. 2b). The shortest of the diagonal distances of the T2 tunnel is 3.78 Å, O(4)–O(4), which is too small to be useful for intercalating any metallic cations. For comparison, the shortest distance for T1 is 4.96 Å, O(5)–O(5).

It is noted that the framework of the title compound and its structural features are similar to that of $Na_xMoP_2O_7$ ($0.25 \leq x \leq 0.5$) (*8*) and $NaMo_2(P_2O_7)_2$ (*9*), differing in lattice origins only, i.e., +(0,0,0.5) and +(0.5,0,0), respectively. In both cases nonstoichiometry was observed owing to the short Na–Na distance between two neighboring sites which are related by the inversion center (i). The lattice origin of the title compound allows a fully occupied strontium cation to be recognized at the special position. Thus the avoidance of a short Sr–Sr distance is observed. Subsequently, a well-behaved strontium atom is refined, as shown by the thermal parameter ($B_{eq}$) for $Sr^{2+}$ ion in Table II.

The structure of $SrV_2(P_2O_7)_2$ can be simply viewed as layers of $VO_6$ octahedra and $P_2O_7$ pyrophosphate groups, alternately stacking along the [−110] direction. The structure of the $[V_2(P_2O_7)_2]^{2-}$ projected along the P(1)–P(2) vector is shown in Fig.

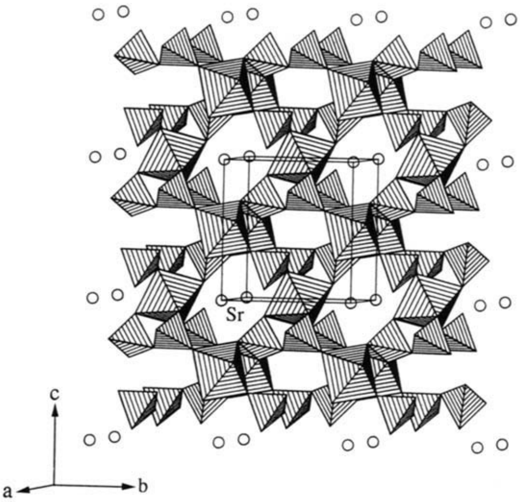

FIG. 1. The STRUPLO-86 polyhedral representation of the extended structure of $SrV_2(P_2O_7)_2$ viewed along the *a*-axis. The triclinic unit cell is outlined. The strontium atoms are represented by open circles.

3. Two types of vanadium metal cations, V(1) and V(2), in the $VO_6$ octahedra are alternately arranged to form an extended layer along the *c* direction. There is no evidence for a direct V–O–V connection between the adjacent $VO_6$ octahedra. However, these octahedra are sharing corner oxygen atoms with the pyrophosphate groups.

A rather short interlayer separation between the two neighboring vanadium layers is observed, $d_L$ = 3.39 Å. The separation is much smaller than the interlayer distances observed in other layered compounds containing the element titanium, e.g., 6.94 and 5.21 Å in $TiP_2O_7$ (*10*), and $BaTi_2(P_2O_7)_2$ (*4*), respectively. This difference in interlayer distances is largely attributed to the bond arrangement between the $MO_6$ octahedra ($M$ = Ti or V) and the $P_2O_7$ groups, and the configuration of the pyrophosphate anion. The P–O–P bond in $TiP_2O_7$ is linear and perpendicular to the $TiO_6$ planes, whereas the P–O–P angle in $BaTi_2(P_2O_7)_2$ is nonlinear. This bent geometry observed in the structure of the latter compound is due to the fact that the terminal oxygen atoms of the same $PO_4$ tetrahedron are bonded to the titanium atoms in two different planes. In the presently studied structure, the different orientation and connectivity of the pyrophosphate groups are obviously responsible for the relatively short interlayer distance.

The basic structure dissimilarity in the compounds associated with trivalent early transition metal cations ($M$) with the general formula $A^{II}M_2(P_2O_7)_2$ is discerned by the structural arrangement between corner-sharing $MO_6$ octahedra and $P_2O_7$ pyrophosphate groups. Both structure types, $BaTi_2(P_2O_7)_2$ and $SrV_2(P_2O_7)_2$, contain two crystallographically different transition metal sites. This originates from the fact that the $MO_6$ octahedra are linked to six or four $P_2O_7$ groups. Essentially the structure framework can be described as being built up from the $M(P_2O_7)_2O_2$ unit (where $M$ = Ti(1) and V(2)), in which two $P_2O_7$ bidentate ligands are sharing corner oxygens with the $MO_6$ octahedron. For the title compound, the two bidentate $P_2O_7$ ligands are bonded to the *trans*-edges of the $VO_6$ octahedron as shown in Fig. 4 of the *trans*-$V(P_2O_7)_2O_2$ unit. In contrast, two $P_2O_7$ ligands in $BaTi_2(P_2O_7)_2$ are bonded to the *cis*-edges of the $TiO_6$ octahedra. This difference in connectivity of the polyhedra and the eclipsed configuration of the pyrophosphate groups (see latter discussion) are attributed to the structural framework accommodation of the smaller electropositive cation.

The bond distances and angles (see Table III) that describe the geometries of the $VO_6$ octahedron and $P_2O_7$ polyhedron are normal and comparable to the values that were previously reported in several other reduced pyrophosphate compounds [(*11*), and references cited therein]. The V–O bond distances range from 1.94 to 2.09 Å, while the terminal P–O bond distances range from 1.49 to 1.54 Å and the bridging P–O range

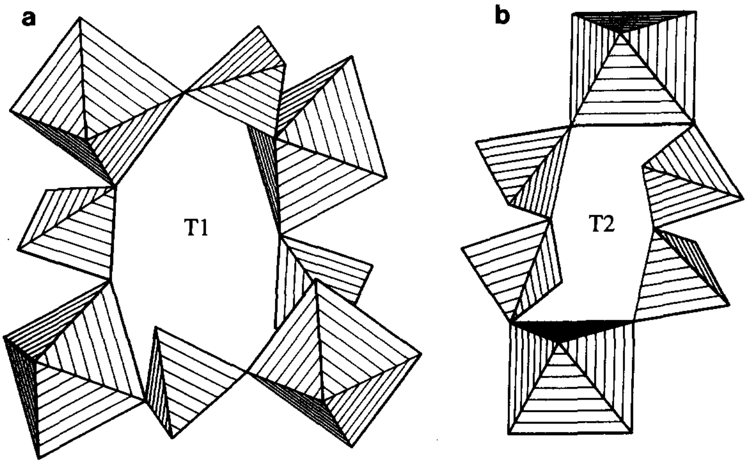

FIG. 2. Projected tunnel structures of (a) strontium site (T1), and (b) empty site (T2). These two sites are centered at (0,0,0) and $(0,\frac{1}{2},\frac{1}{2})$, respectively.

is 1.59–1.61 Å. It is noted that the P–O–P bridging angle, e.g., 132.5°, is on the higher end of the bending angles range. This is due to the steric effect owing to the eclipsed configuration of the $P_2O_7$ polyhedron.

One of the interesting structural features of the title compound rests in its strontium coordination. At first glance, the $Sr^{2+}$ cation forms a slightly distorted $SrO_6$ octahedron with the six Sr–O distances ranging from 2.48 to 2.76 Å. These distances are comparable with the sum of the Shannon crystal radii (based on a six-coordinated $Sr^{2+}$ cation), e.g., 2.58 Å (*12*). Knowing the observed Sr–O distances, the calculated sum of the bond valance (*13*) for the divalent cation results in a low valence number of 1.66. According to Pauling's electrostatic valence rule, the coordination sphere with respect to the $Sr^{2+}$ cation should be increased. This

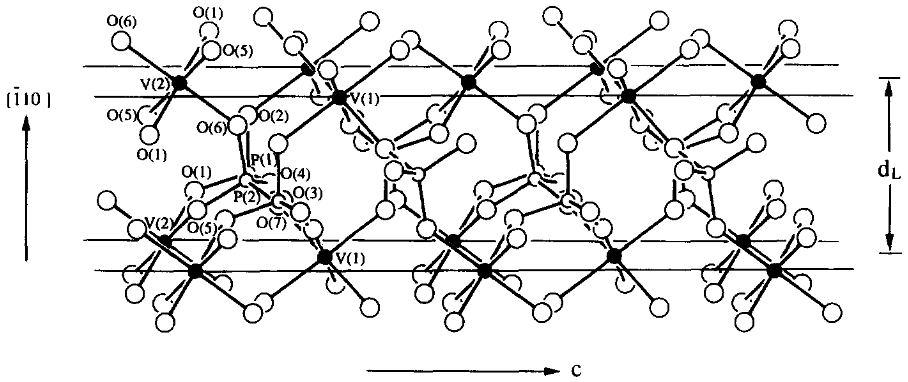

FIG. 3. Stacking of the layers of $VO_6$ octahedra and of pyrophosphate groups in the $[V_2(P_2O_7)_2]^{2-}$ slab is projected approximately along the P(1)–P(2) vector. The small solid and open circles are V and P, respectively. The oxygen atoms are represented by large open circles. The interlayer separation, $d_L$, is 3.39 Å for the title compound, compared to 5.21 Å for $BaTi_2(P_2O_7)_2$ (see text).

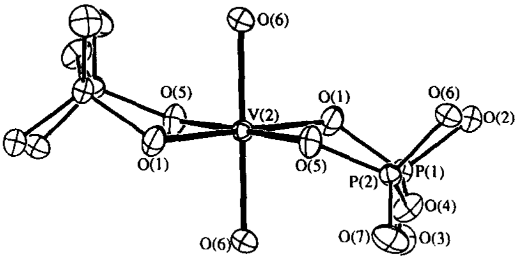

FIG. 4. The ORTEP drawing of the structure of the *trans*-$V(P_2O_7)_2O_2$ unit.

revised geometry includes four additional oxygen atoms from an "outer" sphere coordination with longer Sr–O distances ranging from 3.19 to 3.35 Å. Subsequently, the bond valence calculation indicates a closer value (1.84) to the formal charge of 2+. Therefore, the coordination number for the $Sr^{2+}$ ion should be ten (CN = 10) with six short and four long strontium to oxygen distances (see Table IV). The resulting $SrO_{10}$ polyhedron is then best represented as a tetra-face-capped octahedron, as shown in Fig. 5.

TABLE IV

STRONTIUM TO OXYGEN DISTANCES (Å) AND ANGLES (DEG., OF INNER SPHERE OXYGEN ATOMS) IN $SrO_{10}$ POLYHEDRON

| | | |
|---|---|---|
| $Sr-O(1)^{b,f}$ | 2.761(2) | (2×) |
| $Sr-O(2)^{a,h}$ | 2.592(2) | (2×) |
| $Sr-O(5)^{e,i}$ | 2.481(2) | (2×) |
| $Sr-O(1)^{a,h}$ | 3.347(2) | (2×) |
| $Sr-O(7)^{c,j}$ | 3.185(2) | (2×) |
| $O(1)^b-Sr-O(1)^f$ | 180.00 | |
| $O(2)^a-Sr-O(2)^h$ | 180.00 | |
| $O(5)^e-Sr-O(5)^i$ | 180.00 | |
| $O(1)^b-Sr-O(2)^a$ | 79.65(7) | (2×) |
| $O(1)^b-Sr-O(2)^h$ | 100.35(7) | (2×) |
| $O(1)^f-Sr-O(5)^e$ | 64.22(7) | (2×) |
| $O(1)^b-Sr-O(5)^e$ | 115.78(7) | (2×) |
| $O(2)^h-Sr-O(5)^e$ | 87.65(7) | (2×) |
| $O(2)^a-Sr-O(5)^e$ | 92.35(7) | (2×) |

*Note.* See Table III for symmetry codes, and $h = -1+x, y, -1+z$; $i = -1+x, -1+y, -1+z$; $j = 1-x, -y, -z$.

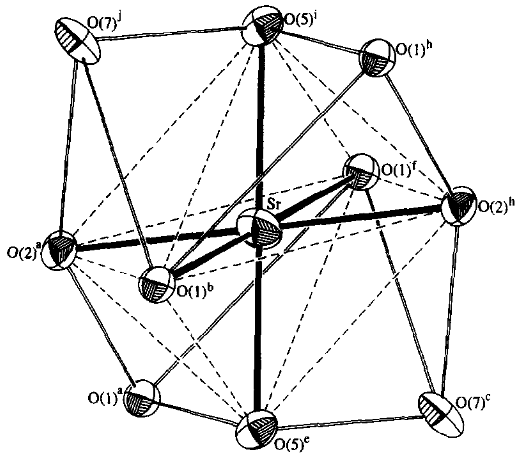

FIG. 5. The tetra-face-capped octahedral representation of $SrO_{10}$. To guide the eyes, the $SrO_6$ octahedral coordination is drawn in thick lines and the triangular faces of the octahedron are outlined with dashed lines. The open lines are drawn to show the face-capping configurations. (See Tables III and IV for the symmetry codes.)

Finally, it should be noted that calcium vanadium(III) pyrophosphate can also be isolated under the same conditions stated above for $SrV_2(P_2O_7)_2$. It is isostructural with $SrV_2(P_2O_7)_2$. For comparison, the indexed cell dimensions (by the single crystal X-ray diffraction method) of $CaV_2(P_2O_7)_2$ are $a = 4.783$ (1) Å, $b = 7.037$ (2) Å, $c = 7.804$ (1) Å, $\alpha = 89.53$ (2)°, $\beta = 92.07$ (2)°, $\gamma = 106.95$ (2)°, $V = 251.1$ (1) Å$^3$.

## Acknowledgments

Acknowledgment is made to the donors of The Petroleum Research Fund, administered by the ACS, for support of this research (Grant ACS-PRF 21154-G3). Financial support, in part, by the National Science Foundation, Solid State Chemistry (SGER), Grant DMR-9012983, is gratefully acknowledged.

## References

1. S. WANG AND S.-J. HWU, unpublished results, Rice University, Houston, TX (1990).
2. A. LECLAIRE, A. BENMOUSSA, M. M. BOREL, A.

Grandin, and B. Raveau, *J. Solid State Chem.* **77,** 299 (1988).

3. S. Wang and S.-J. Hwu, *J. Solid State Chem.* **92,** 219 (1991).
4. S. Wang and S.-J. Hwu, *J. Solid State Chem.* **90,** 31 (1991).
5. E. D. Willis and S.-J. Hwu, unpublished results, Rice University, Houston, TX (1990).
6. PDF, No. 32-1268, JCPDS-International Center for Diffraction Data Swarthmore, PA.
7. C. E. Rice, W. R. Robinson, and B. C. Tofield, *Inorg. Chem.* **15,** 345 (1976).
8. A. Leclaire, M. M. Borel, A. Grandin, and B. Raveau, *Z. Kristallogr.* **184,** 247 (1988).
9. K. H. Lii, J. J. Chen, and S. L. Wang, *J. Solid State Chem.* **78,** 178 (1989).
10. U. Costantino and A. La Ginesta, *Thermochim. Acta* **58,** 179 (1982).
11. K. H. Lii, Y. P. Wang, Y. B. Chen, and S. L. Wang, *J. Solid State Chem.* **86,** 143 (1990).
12. R. D. Shannon, *Act. Crystallogr. Sect. A* **32,** 751 (1976).
13. I. D. Brown and A. Altermatt, *Acta Crystallogr. Sect. B* **41,** 244 (1985).